

# Transactions of The Indian Institute of Metals

Vol. 64, Issues 1 & 2, February-April 2011, pp. 251-254

## Computational modelling of dendritic to globular transition using an isothermal binary phase-field model

**P. Gerald Tennyson and G. Phanikumar**

*Department of Metallurgical and Materials Engineering, IIT Madras, Chennai – 600 036*

*E-mail:* [geraldtennyson@gmail.com](mailto:geraldtennyson@gmail.com)

Received 04 November 2010

Revised 23 December 2010

Accepted 06 January 2011

Online at [www.springerlink.com](http://www.springerlink.com)

© 2011 TIIM, India

**Keywords:**

*phase field model; globularisation; semi solid processing; rheocasting; remelting*

### Abstract

Globular microstructure is suitable for high pressure die casting of semi-solid billets. This is achieved by means of mechanical deformation of the melt or by means of a forced convection in the presence of a thermal gradient. The morphological evolution in an alloy with the starting microstructure as predominantly dendritic is simulated using the phase-field technique. An attempt is made to study the effect of varied thermal profiles that are imposed on the solidified dendrite and the morphological changes effected there upon. Two dimensional simulations are performed for a dilute alloy of a simple lens type phase diagram and the results are presented.

### 1. Introduction

Semi-solid processing (SSP) involves processing metallic alloys between the solidus and liquidus. The most important characteristic of SSP is that the solidification microstructure changes markedly, from dendritic growth under conventional processing conditions to non-dendritic or globular growth [2,3]. Of the many factors that influence the dendritic breakdown, thermal and solutal gradients play a pivotal role in the fragmentation process. Several authors [5-7] have proposed that the thermal gradients in the melt during SSP create an excessive solute pileup at the roots of the dendrite which results in the remelting of the arms at the roots. This along with convection in the melt leads to the formation of globular crystals as the thermal cycling is effected between the solidus and the liquidus [4].

In order to simulate the thermal gradient experienced by a dendrite as it gets stirred between the solidus and the liquidus an appropriate computational model is necessary. Phase field models have gained wide significance in the recent past as it avoids the explicit tracking of the interface. This technique has been extensively used to study microstructure evolution in different situations [8-11]. In this study, an isothermal phase field model for a binary alloy as developed by Warren [12] is used to simulate dendritic growth. The motion of a dendrite during a SSP is captured by imposing thermal cycles on the computational domain. The vertical temperature gradient in a rheocasting setup is captured by the amplitude of the thermal cycle used in the present study. The strength of advection in the rheocasting setup with a linear electromagnetic stirring [8] is conveyed by the wavelength of the thermal cycle imposed in the simulation. In comparison with earlier work by the authors [1], a continuous thermal profile is used rather than a discrete one. Significant changes in the growth morphologies are brought about by changing the amplitude and the duration of the thermal fluctuations. All results described here are for one complete thermal cycle.

### 2. Model

The isothermal binary alloy solidification model developed by Warren et al.[12] is used in this study. It uses a phase field variable  $\phi$ , which is 0 in the liquid and 1 in the solid and varies smoothly between these bulk values within the diffuse interface region.

The governing equation for the phase field  $\phi$  is given by:

$$\frac{\partial \phi}{\partial t} = M_\phi \left[ \varepsilon^2 \nabla^2 \phi - \left( c \frac{\partial f_b}{\partial \phi} - (1-c) \frac{\partial f_a}{\partial \phi} \right) \right] \quad (1)$$

and for the concentration field:

$$\frac{\partial c}{\partial t} = \nabla \cdot \left( M_c c (1-c) \frac{\partial f}{\partial c} \right) \quad (2)$$

where  $M_\phi$  and  $M_c$  are the phase field and concentration mobilities respectively. Anisotropy is included through  $\varepsilon$  in Eq. 1 which is a function of the surface free energy and given by,

$$\varepsilon = \varepsilon(1 + \gamma \cos k\theta) \quad (3)$$

where  $\gamma$  is the strength of anisotropy,  $k$  the mode number (two fold or four fold anisotropy) and  $\theta$  is the orientation of the normal to the interface with respect to the x-axis given by,  $\tan \theta = \phi_y/\phi_x$ . The homogenous free energy density  $f$ , is given by

$$\begin{aligned} f(c, \phi, T) = & (1-c)f_a(\phi, T) + cf_b(\phi, T) + \\ & \frac{RT}{v_m} [c \ln c + (1-c) \ln(1-c)] \end{aligned} \quad (4)$$

where  $f_a$  and  $f_b$  are the free energy densities of the pure components. For further details of the model, the reader is

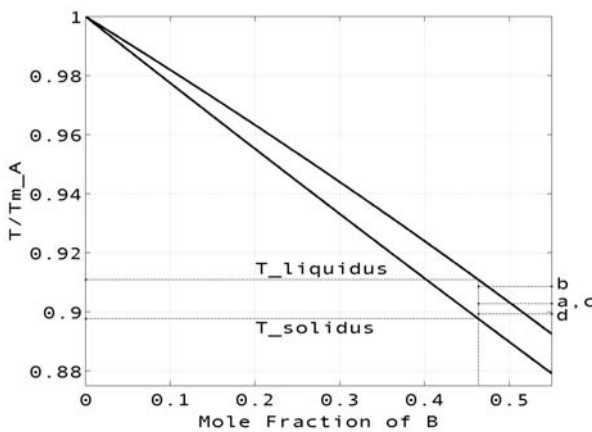


Fig. 1 : A simple lens type phase diagram

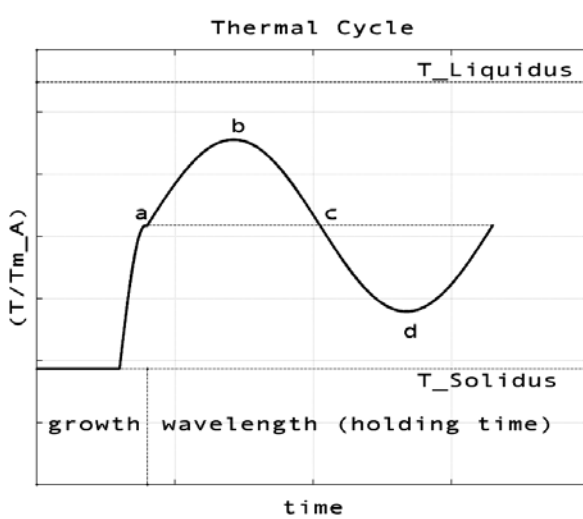
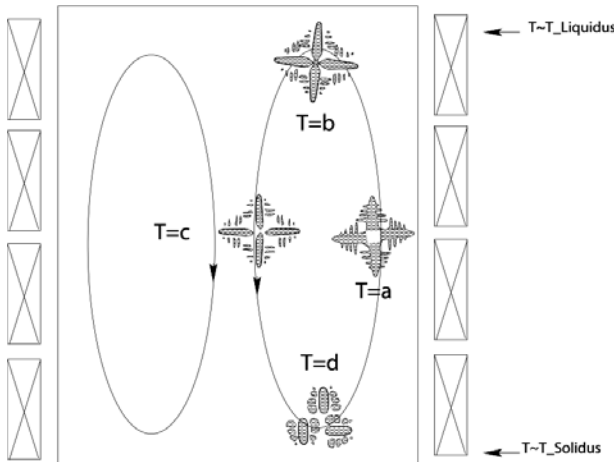


Fig. 2 : (a) Schematic of a SSP setup

Fig. 2 : (b) Thermal profile experienced by the dendrite

directed to references [12, 13].

A simple lens shaped phase diagram as shown in Fig. 1 is used in the present study. Fig. 2a shows the schematic of a SSP setup where a dendrite is made to circulate between the solidus and the liquidus temperature zones due to forced convection. The thermal profile as experienced by this dendrite is depicted in Fig. 2b.

### 3. Numerical simulations

The governing equations for the phase field and concentration were discretized using a finite difference technique. Table 1 lists the various parameters used to simulate dendritic growth.

Table 1 : Phase field parameters used in the study

Grid size	$N_x = N_y$	1000
Melting point of A	$T_m^A$	1.0
Melting point of B	$T_m^B$	0.78
Capillary length	$d_0$	$7.1 \times 10^{-8}$ cm
Diffusivity in the liquid	$D_L$	$1 \times 10^{-5}$ cm <sup>2</sup> /s
Grid spacing	$\Delta x = \Delta y$	$100d_0$
Time step size	$\Delta t$	$0.002 \Delta x^2/D_L$
Specific heat/Latent heat	$C_p/L$	0.002

No flux conditions were applied both for phase and concentration fields. Numerical stability was ensured by satisfying the Neumann stability criterion  $\Delta t \leq \Delta x^2/D_L$ . A dendrite was grown from a square seed placed at left boundary of the domain in an initially undercooled melt, 20K below the liquidus. In order to effectively capture the thermal cycling, the temperature of the domain was increased to point *a* shown in Fig. 1, such that the imposed temperature cycle is well within the solidus and the liquidus. A sinusoidal wave function was chosen for the thermal profile as depicted in Fig. 2b. Table 2 lists the parameters that were employed to simulate the thermal cycling.

The amplitudes  $\Delta T_1$  and  $\Delta T_2$  listed in Table 2, correspond to temperature ranges of 10K and 6K respectively.

Table 2 : Parameters used for the imposed thermal cycle

Amplitude	$\Delta T_1$	0.023
	$\Delta T_2$	0.014
Timesteps	$N_t$	30000, 50000, 70000, 100000
Holding time (wavelength) $\tau = \Delta t N_t$	$\tau_1$	0.0003 s
	$\tau_2$	0.0005 s
	$\tau_3$	0.0007 s
	$\tau_4$	0.001 s

Table 3 : Morphological changes observed for various imposed thermal profiles

	$\tau_1$	$\tau_2$	$\tau_3$	$\tau_4$
$\Delta T_1$	Dendritic	Dendritic	Globular	Globular
$\Delta T_2$	Dendritic	Dendritic	Dendritic	Globular

### 4. Discussion

The amplitude and wavelength of the thermal cycle have a profound impact on the final microstructure. From the thermal profile, when the temperature of the domain is at point *b* (see Fig. 2b), the higher temperature causes the rejection of the solute from the solid as well as the adjoining liquid. As this solute is rejected, lateral transfer of the solute towards the root takes place. This solute pileup brings about

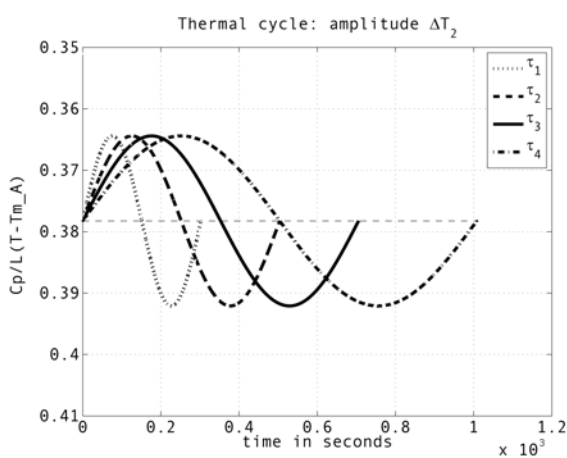
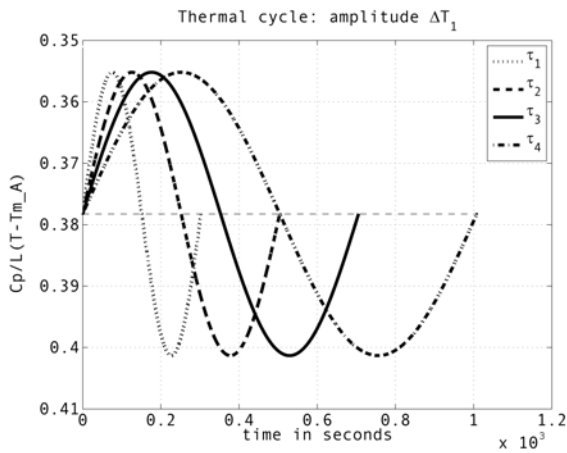
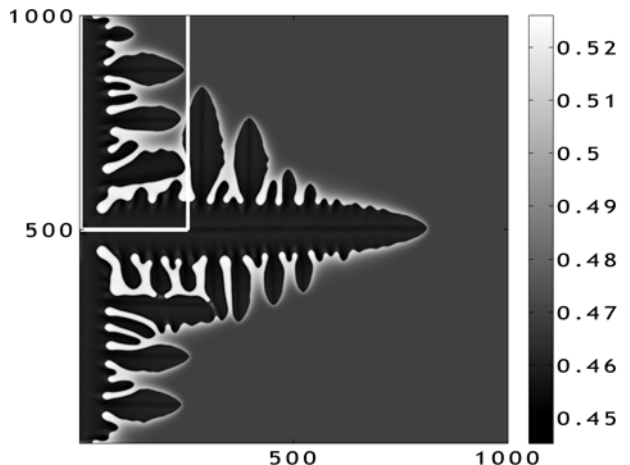
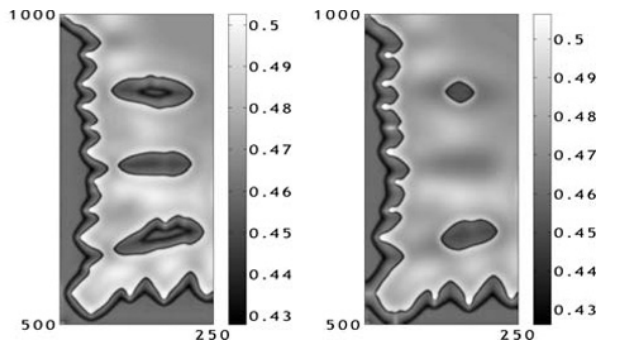
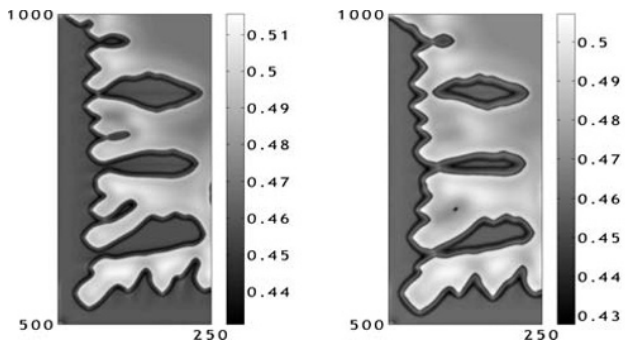
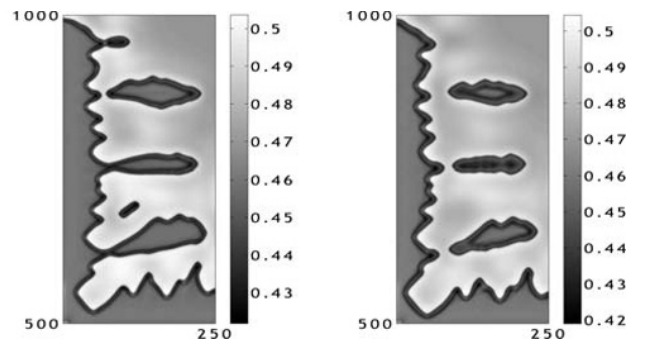
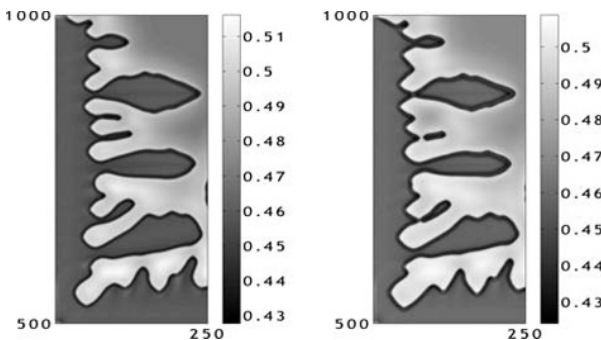
Fig. 3 : (a) Temperature profiles for amplitude  $\Delta T_1$ Fig. 3 : (b) Temperature profiles for amplitude  $\Delta T_2$ 

Fig. 4 : Concentration profile of a dendrite grown isothermally where the inset shows the globular transition at the end of each thermal cycle in Fig. 5

a decrease in the liquidus temperature locally. Hence even though there is a decrease in the temperature at point  $c$ , the solute enriched regions in the vicinity of the roots starts to remelt and gets detached from the primary arm. This process of melting effected by solute enrichment is referred to as solutal remelting [9]. Further decrease in the temperature to point  $d$ , causes an influx of the solute atoms to enter the solid masses that have survived root remelting. Since in this context, morphological changes due to thermal fluctuations are being studied, at the coarsening stage, there is a tendency for the solid masses to grow in an elongated manner due to the surface energy anisotropy. Further dendritic growth from the detached fragments is inhibited due to the imposed thermal cycle.

The temperature profiles for the amplitude  $\Delta T_1$  shown in Fig. 3a, exhibit steeper thermal gradients than that of

Fig. 5 : (a,b,c,d) Composition profiles showing the globular morphology for amplitude  $\Delta T_1$  at the end of thermal cycles,  $\tau_1$ ,  $\tau_2$ ,  $\tau_3$  and  $\tau_4$  respectivelyFig. 5 : (e,f,g,h) Composition profiles showing the globular morphology for amplitude  $\Delta T_2$  at the end of thermal cycles,  $\tau_1$ ,  $\tau_2$ ,  $\tau_3$  and  $\tau_4$  respectively

amplitude  $\Delta T_2$  shown in Fig. 3b. Though the thermal gradient is steep, lesser holding times reduce the possibility for solute accumulation and further remelting and coarsening. This is evident from Fig. 5a and b, wherein no significant morphological changes were observed for  $\tau_1$  and  $\tau_2$ . Alternatively, increased holding times ( $\tau_3$  and  $\tau_4$ ) enhances the possibility for solute pileup at the roots thereby causing root remelting and subsequent coarsening towards a globular microstructure as in Fig. 5c and d. Fig. 5e, f, g and h exhibits a similar situation for  $\Delta T_2$ . Due to the shallow gradient, the duration of holding had to be increased sufficiently to  $\tau_4$  in order to witness the remelting and coarsening effects (see Fig. 5h)

In an earlier work [1], an attempt was made to simulate the dendritic to globular transition involving a discrete thermal profile. Discrete thermal profiles, though emulate isothermal holding conditions, give rise to numerical artifacts like abrupt solute rejection as the thermal gradient imposed goes to infinity. However, such is not the case when a continuous thermal cycle is imposed. Solute rejection and pile up occur in a gradual manner and it more often emulates a practical scenario.

## 5. Conclusions

A phase field model for solidification was used to simulate a dendritic growth isothermally and to demonstrate the effect of dendrite fragmentation in a binary alloy. The globularisation phenomenon was captured effectively by modelling the thermal profile experienced by a free floating

dendrite due to forced convection in a SSP setup. Shallower and much longer holding times tend to favour a more globular microstructure.

## References

1. Gerald Tennyson P, Kumar P, Lakshmi H, Phanikumar G and Dutta P, *Trans Nonferrous Met Soc China*, **20** (2010) s774
2. Flemings MC, *Metall Trans A* **22** (1991) 957
3. Atkinson H V and Liu D, *Mat Sci Eng A*, **496** (2008) 439
4. Tao Li, Xin Lin and Weidong Huang, *Acta Mat*, **54** (2006) 4815
5. Jackson K, Hunt J, Uhlmann D and Seward T, *Trans AIME*, **236** (1966) 149
6. Kattamis T Z, Coughlin J C and Flemings M C, *Trans AIME*, **239** (1967) 1504
7. Fan Z, *Int Mat Rev*, **47** (2002) 49
8. Pramod Kumar, Ph.D. Thesis titled *Experimental investigation of Rheocasting using linear electromagnetic stirring*, Indian Institute of Science, Bangalore, India (2008)
9. Rettenmayr M, Warkentin O, Rappaz M and Exne H E, *Acta Mat*, **49** (2001) 2499
10. Chen L Q, *Annu Rev Mater Res*, **32** (2002) 113
11. Boettigner W J, Warren J A, Beckermann C and Karma A, *Annu Rev Mater Res*, **32** (2002) 163
12. Moelans N, Blanpain B and Wollants P, *Calphad*, **32** (2008) 268
13. Hoyt J J, Asta M and Karma A, *Mat Sci Eng R*, **41**(2003) 121
14. Warren J A and Boettigner W J, *Acta Metall et Mat*, **43** (1995) 689
15. Wheeler A A, Boettigner W J and McFadden G B, *Phys Rev A*, **45** (1992) 7424